Childs Nerv Syst (2011) 27:127–135
DOI 10.1007/s00381-010-1219-6

ORIGINAL PAPER

Analysis of endoscopic third ventriculostomy patency by MRI: value of different pulse sequences, the sequence parameters, and the imaging planes for investigation of flow void

Alp Dinçer · Erdem Yildiz · Saeed Kohan · M. Memet Özek

Received: 14 March 2010 / Accepted: 28 June 2010 / Published online: 15 July 2010

Abstract
Purpose The aim of the study is to evaluate the efficiency of turbo spin-echo (TSE), three-dimensional constructive interference in the steady state (3D CISS) and cine phase contrast (Cine PC) sequences in determining flow through the endoscopic third ventriculostomy (ETV) fenestration, and to determine the effect of various TSE sequence parameters.

Materials and methods The study was approved by our institutional review board and informed consent from all patients was obtained. Two groups of patients were included: group I (24 patients with good clinical outcome after ETV) and group II (22 patients with hydrocephalus evaluated preoperatively). The imaging protocol for both groups was identical. TSE T2 with various sequence parameters and imaging planes, and 3D CISS, followed by cine PC were obtained. Flow void was graded as four-point scales. The sensitivity, specificity, accuracy, positive and negative predictive values of sequences were calculated.
Results Bidirectional flow through the fenestration was detected in all group I patients by cine PC. Stroke volumes through the fenestration in group I ranged 10–160.8 ml/min. There was no correlation between the presence of reversed flow and flow void grading. Also, there was no correlation between the stroke volumes and flow void grading. The sensitivity of 3D CISS was low, and 2 mm sagittal TSE T2, nearly equal to cine PC, provided best result.
Conclusion Cine PC and TSE T2 both have high confidence in the assessment of the flow through the fenestration. But, sequence parameters significantly affect the efficiency of TSE T2.

Presented at RSNA 2007

A. Dinçer (✉) · E. Yildiz
Department of Radiology, School of Medicine,
Acibadem University,
Inonu Cad. Okur Sok. No:21, Kozyatagi,
İstanbul 34742, Turkey
e-mail: adincer@asg.com.tr

S. Kohan
Adult and Pediatric Neurosurgeon, Spinal Surgeon,
St. George Private Hospital and Concord Medical Centre,
Sydney, Australia

M. Memet Özek
Department of Neurosurgery,
Marmara University Medical Center,
Istanbul, Turkey

M. Memet Özek
Division of Pediatric Neurosurgery,
Marmara University Medical Center,
Istanbul, Turkey

M. Memet Özek
Marmara University, Institute of Neurological Sciences,
Istanbul, Turkey

M. Memet Özek
Acıbadem University, School of Medicine,
Istanbul, Turkey

Keywords Endoscopic third ventriculostomy · Fenestration patency · Flow void · TSE · Cine PC

Introduction

Although the role of endoscopic third ventriculostomy (ETV) in patients with hydrocephalus is well established, monitoring patients following this procedure remains controversial [1–4]. Ensuring patency and efficiency of

ventriculostomy is, in particular, difficult in younger patients in whom clinical signs and symptoms of hydrocephalus may be difficult to establish until it reaches critical stages [1]. An objective method for assessment of patency and efficiency of ventriculostomy is an ideal tool for clinicians to ensure favorable outcome. Current magnetic resonance imaging (MRI) criteria such as resolution of periventricular edema, widening of subarachnoid space, demonstration of midsagittal surgical defect of the floor of the third ventricle, or diminish in ventricular size are unreliable in judging the patency of ventriculostomy fenestration; while ventriculography with contrast may be performed, it is invasive and requires ventricular access device [1–3]. So, functional analysis of ventriculostomy patency and the assessment of the procedural success by MRI mainly rely on the demonstration of flow void or flow signal in the floor of the third ventricle [1–12]. Also, the triage of patients with failed ETV solely depends on whether the stoma of ETV is functional or not, since the former requires shunt insertion, while the latter may be explored for redo ETV [6, 11]. Although various motion-sensitive MRI techniques (SE: spin-echo, TSE: turbo spin-echo, SSFP: steady state free precession, 3D CISS: three-dimensional constructive interference in the steady state, PSIF: reverse fast imaging with steady state precession, SPAMM: spatial modulation of magnetization, cine PC: cine phase contrast) have been applied, 3D CISS, TSE, and cine PC have gained acceptance in evaluating the flow through the fenestration [4, 7, 9, 10, 12–16]. However, there is no consensus on the reliability of TSE and 3D CISS to demonstrate flow through the fenestration in the literature [1, 12–15]. Furthermore, although in a phantom study, the effect of the parameters of spin-echo sequence on the flow void phenomenon have been reported, to our knowledge there is no report concerning in vivo study in this setting so far [17].

The aim of this study is to evaluate the efficiency of TSE, 3D CISS, and cine PC sequences in determining the patency and flow through ventriculostomy fenestration. Furthermore, we aim to determine the effect of various TSE sequence parameters (including slice thickness, flow compensation gradient, the number of averages, receiver bandwidth, and the imaging planes) on the accuracy of this technique for assessment of ETV patency.

Method and material

Subjects

The study was approved by our institutional review board, and we obtained informed consent from all patients or caregivers. We included two groups of patients prospectively in the study. Group I included 24 consecutive patients (19 males/5 females, mean age 8 years, age range 9 months–31 years) who were followed-up after ETV with "good" clinical outcome from Jan 2005 to May 2007. The "good" clinical outcome was defined as the resolution of clinical symptoms and signs of increased intracerebral pressure prior to ETV, or slowing of the head circumference growth rate. Obstructive hydrocephalus was diagnosed in all, but four patients. In ten patients, the cause was primary aqueduct stenosis; four with membranous obstruction of fourth ventricle exit foramina (three of them also have cisternal obstructive membranes); four patients with secondary stenosis due to tectal tumor; one patient with Chiari type 2 malformation, and one with arachnoid cyst. ETV was performed as the primary procedure in 19 patients and as secondary procedure due to shunt failure in the other five patients. The follow-up MRI was performed between 2 and 24 months (mean 18.5 months) after the ETV procedure. Group II included 22 patients (16 males/6 females; mean age 6.2 years, age range 3 months to 37 years) as control who were evaluated with MRI preoperatively for etiology of hydrocephalus from Jan 2005 to May 2007. The second group was used to evaluate the preoperative pattern of flow void phenomenon near the third ventricle in the presence of hydrocephalus prior to ETV, in order to assess the false positive and true negative situations. This group consisted of 11 primary aqueduct stenosis cases, five secondary aqueduct stenosis cases due to tumor of tectal plate, three fourth ventricular outlet obstruction (two of them also have cisternal membranous obstruction) cases, and three communicating hydrocephalus cases.

MR imaging technique

All MR studies were performed with a 3 T System using an eight-channel head coil (Siemens, Erlangen). All patients younger than 10 years were examined routinely under sedation. The imaging protocol for both groups was nearly identical. Axial TSE T2 (5 mm section thickness without flow compensation), sagittal TSE T2 (5 mm section thickness with flow compensation), sagittal TSE T2 (2 mm section thickness with flow compensation), sagittal TSE T2 (2 mm section thickness without flow compensation), coronal TSE T2 (3 mm section thickness with flow compensation and chemical fat saturation), axial TSE T1, and sagittal 3D Turbo fast low angle shot (TurboFLASH) T1, and sagittal 3D CISS, followed by sagittal or axial-oblique cine phase contrast (cine PC) were obtained. The various sequence parameters are summarized in Table 1.

3D CISS sequence was applied in midline sagittal plane with the following parameters: time of repetition (TR), 10.94 ms; time of echo (TE), 5.47 ms; flip angle, 500; field of view (FOV), 200×180 mm; matrix, 320×320; band-

Table 1 MR imaging sequences parameters

Sequences	TR (ms)	TE (ms)	ETL	BW (hertz/pixels)	Interslice gap (%)	Spatial resolution (mm^3)	Flow compensation	Number of averages	Time of acquisition (minutes)
5 mm axial TSE T2 w/o FC	3,590	101	9	100	20	1.75 (0.7×0.5×5)	–	2	1.53
5 mm sagittal TSE T2 w FC	5,590	103	13	171	20	2.25 (0.9×0.5×5)	Read	1	1.01
2 mm sagittal TSE T2 w/o FC	3,000	131	13	100	10	1.20 (1×0.6×2)	–	2	1.41
2 mm sagittal TSE T2 w FC	2,200	97	13	300	10	1.20 (1×0.6×2)	Read	4	2.25
3 mm coronal TSE T2 w FC	4,710	124	13	121	25	1.08 (0.9×0.4×3)	Read	1	1.36
Sagittal 3D CISS	10.9	5.5	0	130	0	0.22 (0.6×0.6×0.6)	–	1	4.48
Sagittal TurboFLASH T1	2,000	3.9	0	130	0	0.51 (0.8×0.8×0.8)	–	1	4.14

TR time of acquisition, *TE* time of echo, *ETL* echo train length, *BW* bandwidth, *TSE* turbo spin-echo, *w* with, *w/o* without, *FC* flow compensation gradient, *CISS* constructive interference in the steady state, *TurboFLASH* turbo fast low angle shot

width, 130 Hz/pixels; partition/slap thickness, 0.6/28.8 mm; partition number, 48; measurement, one. While sagittal 5 mm section thickness T2, 3 mm section thickness coronal TSE T2, and axial 5 mm section thickness T2 cover the whole brain, thin section TSE T2 images were only applied on parasagittal and midsagittal areas, including whole cisterns and fourth ventricle outlets.

The sequence parameters of the midline high-resolution sagittal cine PC were as follows: TR, 37 ms; TE, 5.6 ms; averages, three; FOV, 216×240 mm; slice thickness, 2 mm; flip angle, 30°; matrix, 256×256; voxel size, 0.9×0.9×2 mm^3; velocity encoding, 20 cm/s; direction of flow encoding, foot to head; and bandwidth, 391 Hz/Px. Electrocardiogram or pulse trigger was used with 90% acquisition window. Axial-oblique cine PC was obtained with the same parameters except the velocity encoding direction, which was set to the through plane. Imaging plane was perpendicular to the floor of the third ventricle in group I and perpendicular to cerebral aqueducts in group II. Measurement time was approximately 2–4 min for each sequence according to the heart rate. Cine PC was evaluated with vendor supplied commercially available software (Argus on a Leonardo workstation, Siemens, Erlangen).

Quantitative assessment of the flow void

The flow void adjacent to the third ventricle was interpreted on axial TSE T2 (5 mm section thickness without flow compensation), sagittal TSE T2 (5 mm section thickness with flow compensation), sagittal TSE T2 (2 mm section thickness with flow compensation), sagittal TSE T2 (2 mm section thickness without flow compensation), coronal TSE T2 (3 mm section thickness with flow compensation and chemical fat saturation), and sagittal 3D CISS images on consensus by two experienced radiologists (A.D., 17 years experience in neuroradiology; E.Y., 7 years experience in neuroradiology). Every sequence was interpreted randomly at different sessions.

The flow void phenomenon near the third ventricle was classified into four categories, both in groups I and II for all sequences: grade 0 (no flow void in the interpeduncular cistern, through the floor of the third ventricle or inside the third ventricle); grade 1 (flow void in only one of them); grade 2 (flow void in two of them); grade 3 (flow void in all of them) (Figs. 1 and 2).

CSF flow through the stoma in group I patients was confirmed qualitatively with demonstration of biphasic flow through the stoma using sagittal and axial-oblique cine PC sequence, where phase images were displayed in closed loop cine format.

CSF flow quantification through the fenestration

High-resolution axial-oblique cine PC was used for CSF flow quantification through the stoma in group I patients. Axial-oblique true phase images were processed for quantification. Using vendor-supplied standard software (Argus on Leonardo VD10B), a spherical region of interest was placed covering the whole stoma adequately shown on a magnified image where CSF flow and velocity waveforms were generated. The direction of the flow during the diastole and systole through the fenestration was determined. Stroke volume was calculated, as described in the literature [4, 18].

Statistical analysis

After grading of each sequence, the sensitivity, the specificity, the accuracy, the positive predictive value, and

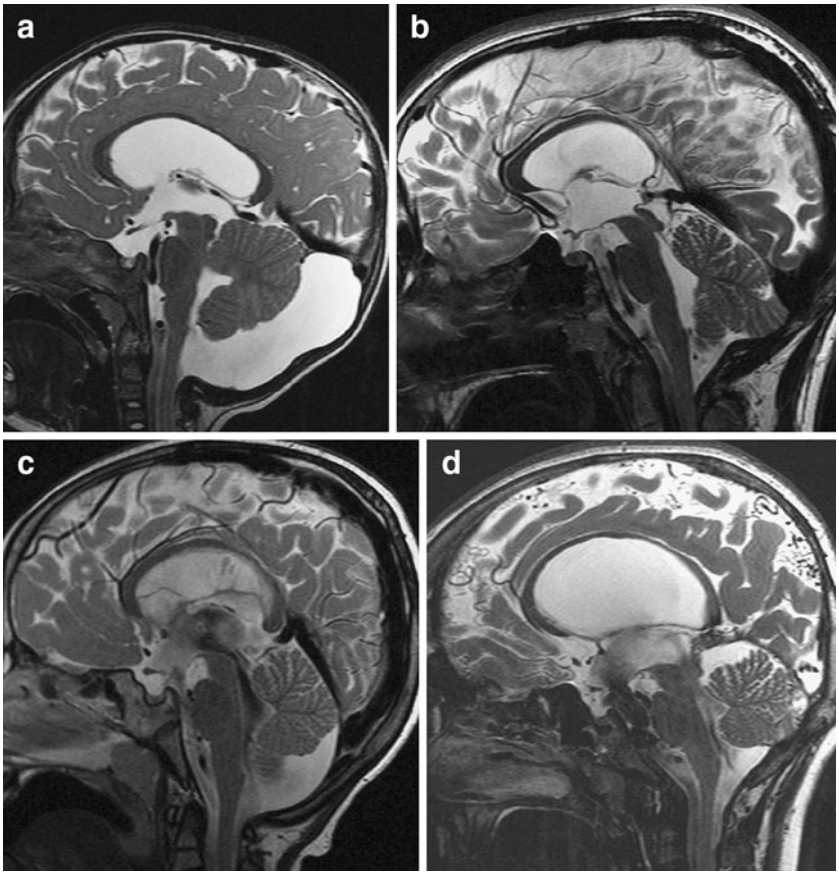

Fig. 1 **a** There is no clear signal void through the floor of the third ventricle in a patient with ETV in the midsagittal image of 5 mm thickness sagittal TSE. Flow void is graded as grade 0. **b** There is signal void only in the interpeduncular and prepontine cisterns, not through the floor of the third ventricle and inside the third ventricle in a patient evaluated for hydrocephalus prior to surgery. Flow void is graded as grade 1 in sagittal 2 mm TSE T2. **c** A patient with communicant hydrocephalus after ETV demonstrates flow through the floor of the third ventricle and prepontine cistern in 2 mm sagittal TSE T2 with flow compensation. Flow void is graded as grade 3. **d** There is extensive flow void graded as grade 3 through the fenestration in sagittal TSE T2 without flow compensation

the negative predictive value of each sequence for flow void were calculated as follows (TP, true positive; TN, true negative; FP, false positive; FN, false negative):

$$\text{Sensitivity} = \frac{TP}{TP+FN}$$

$$\text{Specificity} = \frac{TN}{TN+FP}$$

$$\text{Accuracy} = \frac{TP+TN}{TP+TN+FP+FN}$$

$$\text{Positive predictive value} = \frac{TP}{TP+FP}$$

$$\text{Negative predictive value} = \frac{TN}{TN+FN}$$

Grades 2 and 3 flow voids in group I patients are interpreted as true positive. Grades 0 and 1 flow void in group I patients are treated as false negative. Grades 0 and 1 flow void in group II patients are considered as true negative. Grades 2 and 3 flow void in group II patients are interpreted as false positive.

Results

The values of flow quantification and the flow void grading of each sequence for each patient in group I are demonstrated in Table 2. While bidirectional flow through the stoma was detected in all group I patients by cine PC, no biphasic flow was seen through the floor of the third ventricle in group II patients. Stroke volumes through the stoma in group I patients ranged 10–160.8 ml/min (mean 61.62 ml/min). Reversed flow circulation (craniocaudal in diastole, caudocranial in systole) at the ventriculostomy was observed in nine patients (37.5%). There was no correlation between the presence or absence of reversed flow and the flow void grading of MRI sequences. Also, there was no correlation between the amount of stroke volume and the flow void grading of all MRI sequences.

The grade 2 or 3 flow void at the ventriculostomy stoma was determined in all sequences and imaging planes in all group I patients with stroke volume values higher than 52 ml/min. In 5 mm sagittal T2 and 3 mm coronal T2, the stroke volume was always higher than 52 ml/min if grade 2 or 3 flow void was seen at the ventriculostomy.

Flow void grading in group II patients is demonstrated in detail in Table 3. As all the sequences obtained in the control group (group II) demonstrated grade 1 flow void (ranged 3 to 12 out of 22 patients) which could be related to vascular or CSF pulsation, grades 0 and 1 were taken as flow negative, while grades 2 and 3 were accepted as flow positive.

The results of flow void grades on postoperative MRI for the group I patients are shown in Table 4.

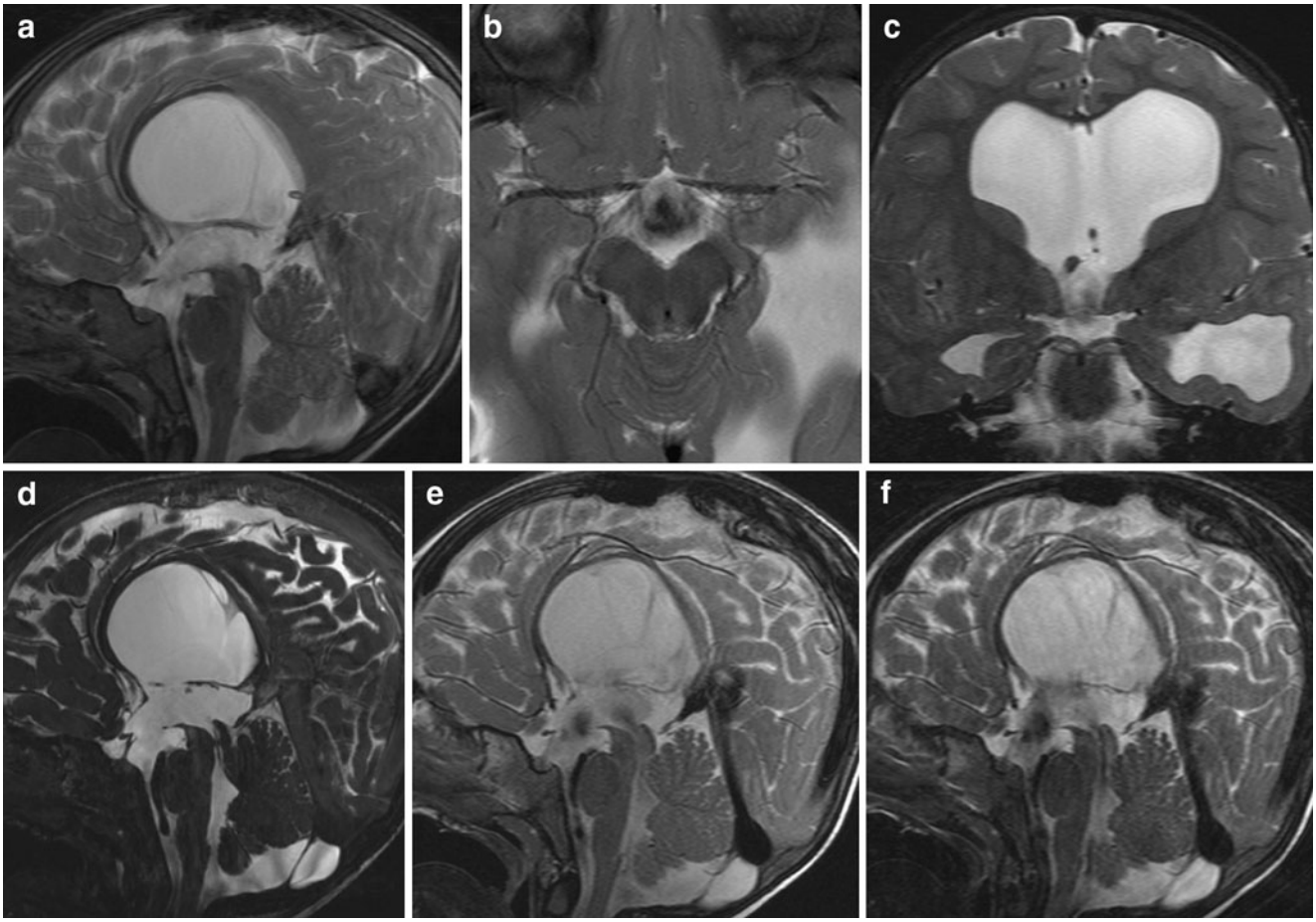

Fig. 2 **a** 5 mm sagittal TSE T2 obtained 12 months after ETV demonstrates surgical defect in the floor of the third ventricle of a 22-month-old boy with communicant hydrocephalus. Although there is slight heterogeneity in the interpeduncular cistern and the third ventricle, flow void is not seen as definite hypointensity in them. Flow void is graded as grade 0 in midsagittal 5 mm sagittal TSE T2, **b** 5 mm axial TSE T2 through the interpeduncular cistern demonstrates extensive signal void in the interpeduncular cistern. As flow void also is seen in two consecutive slices through the floor of the third ventricle and in the third ventricle (not shown), it is graded as grade 3, **c** 3 mm coronal TSE T2 demonstrate grade 2 flow void as seen in the third ventricle and through the fenestration, but not in the interpeduncular cistern, **d** sag 3D CISS demonstrates no flow void in cisterns, through the fenestration and in the third ventricle. It is graded as grade 0, **e** 2 mm sagittal TSE T2 with flow compensation shows flow void obviously in the third ventricle and through the fenestration. It is graded as grade 2, and **f** 2 mm sagittal TSE T2 without flow compensation shows extensive grade 3 flow void in the interpeduncular cistern, through the fenestration and in the third ventricle

The statistical parameters for each MRI sequence were calculated as described in "material and method" section for flow void as shown in Table 5. Five mm sagittal TSE T2 with flow compensation had the least sensitivity in demonstration of flow void phenomenon, while showing very high specificity. It demonstrated flow void in only 12 out of 24 patients with ETV. The sensitivity of 3D CISS was relatively low compared with the other sequences, only exceeding 5 mm sagittal TSE T2 with flow compensation. But, it has also very high specificity. Both 2 mm sagittal TSE T2 with or without flow compensation had very high sensitivity, specificity, accuracy, positive predictive value, and negative predictive value. Two mm sagittal TSE T2 without flow compensation showed flow void in all of group I patients. Five mm axial TSE T2 had high sensitivity, but relatively low specificity. On the contrary, 3 mm coronal TSE T2 with flow compensation had low sensitivity, and high specificity compared to other sequences.

Discussion

Since the follow-up of patients with ETV rely mainly on demonstration of flow or flow void through the fenestration, the methodology which is used to judge this finding has crucial importance. Various MRI sequences have been applied to this problem. Jack and Kelly first assessed the patency of ETV with spin-echo T2-weighted images and demonstrated that an anterior/inferior third ventricular flow

Table 2 The values of flow quantifications and the flow void grading of sequences for each patient in group I

	The values of flow quantification		The flow void grading of MRI sequences					
Patient number	Stroke volume	Reversed flow	5mm sagittal T2 w FC	5mm axial T2 w/o FC	2mm sagittal T2 w/o FC	2mm sagittal T2 w FC	3mm coronal T2 w FC	0.6mm sagittal 3D CISS
1	15.6	1	0	2	2	2	1	3
2	30.7	0	1	2	3	3	3	0
3	18.9	1	1	3	3	3	2	3
4	71.5	1	2	3	3	2	3	2
5	33.12	0	1	3	3	3	3	2
6	104.56	1	3	3	3	3	3	3
7	52	1	1	3	3	3	2	1
8	10	0	1	3	3	3	0	1
9	43.27	1	1	2	3	2	1	0
10	44.88	0	1	3	3	2	1	0
11	111.38	1	2	3	3	3	3	3
12	22.46	0	0	3	3	3	0	3
13	47.46	0	1	3	3	3	3	3
14	100.07	0	3	3	3	3	3	3
15	160.8	0	3	3	3	3	3	2
16	77.06	1	3	3	3	3	3	3
17	114.8	0	3	3	3	3	3	3
18	46.64	1	2	3	3	3	3	2
19	97.52	0	3	3	3	3	3	3
20	25.38	0	0	2	2	1	1	3
21	50.26	0	1	3	3	2	2	0
22	97.51	0	3	3	3	3	3	3
23	39.3	0	3	3	3	3	2	1
24	63.6	0	3	3	3	3	3	3

TSE turbo spin-echo, *w* with, *w/o* without, *FC* flow compensation gradient, *3D CISS* three-dimensional constructive interference in the steady state

void was indicative of a functioning ETV [9]. Wilcock et al. first used TSE sequence to evaluate patients with ETV [12]. Although, in nearly almost every publication concerning follow-up and assessment of fenestration patency, TSE have been included as a part of study, there is no consensus about its validity in that setting [1, 2, 4, 12–14]. Although Malko et al. demonstrated that flow void is strongly dependent on echo time, as well as some other sequence parameters such as slice thickness and field of view that may affect the appearance of flow void in spin-echo

Table 3 Analysis of preoperative MRI for flow void grades in group 2 patients

Grades of flow void	5mm sagittal TSE T2 w FC	5mm axial TSE T2 w/o FC	3mm coronal TSE T2 w FC	0.6mm sagittal 3D CISS	2mm sagittal TSE T2 w/o FC	2mm sagittal TSE T2 w FC	Total
0	18	8	15	19	10	10	80
1	4	9	7	3	11	12	46
2	0	2	0	0	1	0	3
3	0	3	0	0	0	0	3
Total	22	22	22	22	22	22	132

TSE turbo spin-echo, *w* with, *w/o* without, *FC* flow compensation gradient, *3D CISS* three-dimensional constructive interference in the steady state

Table 4 Analysis of postoperative MRI sequences for flow void in group I patients

Grades of flow void	5mm sagittal TSE T2 w FC	5mm axial TSE T2 w/o FC	3mm coronal TSE T2 w FC	0.6mm sagittal 3D CISS	2mm sagittal TSE T2 w/o FC	2mm sagittal TSE T2 w FC	Total
0	3	0	2	4	0	0	9
1	9	0	4	3	0	1	17
2	3	4	4	4	2	5	22
3	9	20	14	13	22	18	96
Total	24	24	24	24	24	24	144

TSE turbo spin-echo, *w* with, *w/o* without, *FC* flow compensation gradient, *3D CISS* three-dimensional constructive interference in the steady state

sequence, there has been no published correlative study which investigated the effect of operator-dependent sequence parameters of TSE sequence in vivo so far [17]. Furthermore, the sequence parameters of TSE in these studies were not described in detail. Cine PC technique has been extensively studied to document the patency of ETV [1, 3–8, 10, 11, 14]. These studies confirmed that cine PC sequence could be effectively used in that setting. Since it is extremely sensitive to membrane in the cisterns, 3D CISS sequence has gained acceptance in both preoperative and postoperative evaluation of patients with ETV [13, 15, 18]. Albeit, it has inherent disability to demonstrate flow in the cistern, some reports advocated its usage to investigate flow void through the fenestration [15]. Other MRI techniques such as SSFP, PSIF and SPAMM offer some advantages in the demonstration of flow or flow void, but they have not gained wide acceptance [14, 16].

Our study has three main findings: (1) it demonstrates that cine PC is a reliable qualitative and quantitative technique for flow through the fenestration and could be used as a criterion standard, as stated in the literature. (2) 3D CISS is less sensitive, comparing TSE with the combination of various sequence parameters to demonstrate flow void. (3) TSE, with proper sequence parameters and imaging planes, is nearly equal to cine PC in the assessment of flow through the fenestration qualitatively.

Cine PC

With high spatial resolution cine PC, we could show biphasic flow through the fenestration in every patient with good clinical outcome after ETV, whereas, there was no biphasic flow near the third ventricle in control subjects. Furthermore, we could quantify the flow through the fenestration and determine the directionality of the flow. However, the range of stroke volumes of the fenestration in our patients is wide. So, we could not identify a cut off value which may help us to assess the outcome of the patients after ETV. Also, we could not observe any relationship between the values of stroke volume, the directionality of flow through the fenestration, and the visibility of flow void phenomenon in any sequence and sequence parameters.

3D CISS

3D CISS is extremely important in the preoperative evaluation of hydrocephalus and in the decision making process [13, 15, 18]. Furthermore, it showed excellent demonstration of the

Table 5 Statistical parameters for each MRI sequence for flow void

	5mm sagittal TSE T2 w FC (%)	5mm axial TSE T2 w/o FC (%)	3mm coronal TSE T2 w FC (%)	0.6mm sagittal 3D CISS (%)	2mm sagittal TSE T2 w/o FC (%)	2mm sagittal TSE T2 w FC (%)
Sensitivity	50	100	75	71	100	96
Specificity	100	77	100	100	95	100
Accuracy	74	90	87	85	98	98
Negative predictive value	65	100	79	76	100	96
Positive predictive value	100	83	100	100	96	100

TSE turbo spin-echo, *w* with, *w/o* without, *FC* flow compensation gradient, *3D CISS* three-dimensional constructive interference in the steady state

surgical defect. However, it is hard to say that it could be successful in the assessment of functional status of the fenestration due to its low sensitivity to flow void phenomenon compared to the other sequences.

TSE

TSE sequence has been the basic MRI sequence since its description [19, 20]. It is fast, widely available, and easy to implement. However, optimal clinical application of TSE pulse sequences requires careful attention to selection of imaging parameters, and it is more prone to flow-related artifact [19–23]. Fortunately, this feature enables us to assess flow and related issues. Washing out and intravoxel dephasing of protons cause signal loss which is called "flow void". Some strategies have been introduced to suppress or enhance the flow-related artifact and flow void in TSE sequence such as flow compensation, implementation of presaturation pulse, and changing the phase-frequency encoding directions [19, 21, 23–25]. Also, it has been known that some operator-dependent sequence parameters such as time of echo, slice thickness, spatial resolution, receiver bandwidth, the number of average, and echo train length could affect the flow- related artifact or flow void phenomenon. Although common usage of TSE, marked sensitivity to flow, and the theoretical effect of sequence parameters of TSE on flow-related artifact and flow void phenomenon, to the best of our knowledge, there has not been any publication that investigates the effects of sequence parameters on flow void phenomenon to assess flow through the ETV fenestration [22, 23, 25]. In the clinical setting, we investigated some important operator-dependent parameters such as the effect of flow compensation gradient, slice thickness, spatial resolution, receiver bandwidth, the number of acquisition, and imaging planes on flow void in TSE, comparing 3D CISS and cine PC. On the other hand, we could not investigate all parameters in a single experiment for a practical reason. It seems that the section thickness and imaging planes is the most effective operator-dependent parameter of TSE sequences, as the thinner the slice, the more enhanced the visibility of flow void. Axial 5 mm TSE T2 is an exception with high sensitivity to flow void. This could be explained by the perpendicularity between the flow direction and the imaging plane. Unfortunately, axial imaging plane also enhances every kind of flow-related artifact in the cisterns, as well as flow through the fenestration, resulting in a decreased specificity. "Loss of phase coherence in spins having constant velocities can be recovered with the addition of gradient waveform lobes known as first order gradient moment nulling or flow compensation. But, it has no theoretical impact on pulsatile flow such as flow through the third ventricle stoma. In our cases, although there is a minor variation in the grading of flow void between the sequences with or without flow compensation, there is no statistical differences between 2 mm sagittal TSE T2 with or without flow compensation in terms of whether flow void is present or not". Two mm sagittal TSE T2 with or without flow compensation demonstrates flow void nearly equal to cine PC with high sensitivity, specificity, and accuracy.

Conclusion

The assessment of flow through the fenestration after ETV has crucial importance and plays an important role in the decision making process. Although various MR imaging sequences have been implemented to demonstrate it, TSE T2, 3D CISS, and cine PC are preferred. Our study demonstrates that TSE T2 and cine PC are most useful in the assessment of flow through the fenestration, but 3D CISS is not. Furthermore, the proper demonstration of flow through the fenestration with TSE T2 depends strongly on appropriate selection of sequence parameters and imaging planes. Sagittal TSE T2 with 2-mm slice thickness provides prompt and robust qualitative evidence for existence of flow through the fenestration.

Conflict of interest The authors declare that they have no conflict of interest.

Disclosure The authors have no disclosure.

References

1. Fischbein NJ, Ciricillo SF, Barr RM, McDermott M, Edwards MS, Geary S, Barkovich AJ (1998) Endoscopic third ventriculocisternostomy: MR assessment of patency with 2-D cine phase-contrast versus T2-weighted fast spin echo technique. Pediatr Neurosurg 28:70–78
2. Joseph VB, Raghuram L, Korah IP, Chacko AG (2003) MR ventriculography for the study of CSF flow. AJNR 24:373–381
3. Kim SK, Wang KC, Cho BK (2000) Surgical outcome of pediatric hydrocephalus treated by endoscopic III ventriculostomy: prognostic factors and interpretation of postoperative neuroimaging. Childs Nerv Syst 16:161–168
4. Bargallo N, Olondo L, Garcia AI, Capurro S, Caral L, Rumia J (2005) Functional analysis of third ventriculostomy patency by quantification of CSF stroke volume by using cine phase-contrast MR imaging. AJNR 26:2514–2521
5. Feng H, Huang G, Liao X, Fu K, Tan H, Pu H, Cheng Y, Liu W, Zhao D (2004) Endoscopic third ventriculostomy in the management of obstructive hydrocephalus: an outcome analysis. J Neurosurg 100:626–633
6. Fukuhara T, Luciano MG, Kowalski RJ (2002) Clinical features of third ventriculostomy failures classified by fenestration patency. Surg Neurol 58:102–110

7. Fukuhara T, Vorster SJ, Ruggieri P, Luciano MG (1999) Third ventriculostomy patency: comparison of findings at cine phase-contrast MR imaging and at direct exploration. AJNR 20:1560–1566
8. Hopf NJ, Grunert P, Fries G, Resch KD, Perneczky A (1999) Endoscopic third ventriculostomy: outcome analysis of 100 consecutive procedures. Neurosurgery 44:795–804
9. Jack CR Jr, Kelly PJ (1989) Stereotactic third ventriculostomy: assessment of patency with MR imaging. AJNR 10:515–522
10. Lev S, Bhadelia RA, Estin D, Heilman CB, Wolpert SM (1997) Functional analysis of third ventriculostomy patency with phase-contrast MRI velocity measurements. Neuroradiology 39:175–179
11. Mohanty A, Vasudev MK, Sampath S, Radhesh S, Sastry Kolluri VR (2002) Failed endoscopic third ventriculostomy in children: management options. Pediatr Neurosurg 37:304–309
12. Wilcock DJ, Jaspan T, Worthington BS, Punt J (1997) Neuro-endoscopic third ventriculostomy: evaluation with magnetic resonance imaging. Clin Radiol 52:50–54
13. Aleman J, Jokura H, Higano S, Akabane A, Shirane R, Yoshimoto T (2001) Value of constructive interference in steady-state three-dimensional, Fourier transformation magnetic resonance imaging for the neuroendoscopic treatment of hydrocephalus and intracranial cysts. Neurosurgery 48:1291–1295, discussion 1295–1296
14. Connor SE, O'Gorman R, Summers P, Simmons A, Moore EM, Chandler C, Jarosz JM (2001) SPAMM, cine phase contrast imaging and fast spin-echo T2-weighted imaging in the study of intracranial cerebrospinal fluid (CSF) flow. Clin Radiol 56:763–772
15. Doll A, Christmann D, Kehrli P, Abu Eid M, Gillis C, Bogorin A, Thiebaut A, Dietemann JL (2000) Contribution of 3D CISS MRI for pre- and post-therapeutic monitoring of obstructive hydrocephalus. J Neuroradiol 27:218–225
16. Hoffmann KT, Lehmann TN, Baumann C, Felix R (2003) CSF flow imaging in the management of third ventriculostomy with a reversed fast imaging with steady-state precession sequence. Eur Radiol 13:1432–1437
17. Malko JA, Hoffman JC Jr, McClees EC, Davis PC, Braun IF (1998) A phantom study of intracranial CSF signal loss due to pulsatile motion. AJNR 9:83–89
18. Dincer A, Kohan S, Ozek MM (2009) Is all "communicating" hydrocephalus really communicating? Prospective study on the value of 3D-constructive interference in steady state sequence at 3 T. AJNR 30(10):1898–1906
19. Low RN, Hinks RS, Alzate GD, Shimakawa A (1994) Fast spin-echo MR imaging of the abdomen: contrast optimization and artifact reduction. J Magn Reson Imaging 4:637–645
20. Hennig J, Friedburg H (1988) Clinical applications and methodological developments of the RARE technique. Magn Reson Imaging 6:391–395
21. Jolesz FA, Jones KM (1993) Fast spin-echo imaging of the brain. Top Magn Reson Imaging 5:1–13
22. Mulkern RV, Wong ST, Winalski C, Jolesz FA (1990) Contrast manipulation and artifact assessment of 2D and 3D RARE sequences. Magn Reson Imaging 8:557–566
23. Stark DD, Hendrick RE, Hahn PF, Ferrucci JT Jr (1987) Motion artifact reduction with fast spin-echo imaging. Radiology 164:183–191
24. Jones KM, Mulkern RV, Schwartz RB, Oshio K, Barnes PD, Jolesz FA (1992) Fast spin-echo MR imaging of the brain and spine: current concepts. AJR 158:1313–1320
25. Li T, Mirowitz SA (2003) Fast T2-weighted MR imaging: impact of variation in pulse sequence parameters on image quality and artifacts. Magn Reson Imaging 21:745–753